The Upgraded Summing NaI(Tl) (SuN++) Absorption Spectrometer

E. K. Ronning[a,b], S. Uthayakumaar[a], A. Spyrou[a,c], A. L. Richard[a,d], S. N. Liddick[a,b], A. Tsantiri[a,c], R. Ringle[a], H. Arora[e], H. C. Berg[a,c], J. M. Berkman[a,b], D. L. Bleuel[f], K. Bosmpotinis[a,c], S. E. Campbell[a,c], X. Chen[a], B. P. Crider[g], R. J. Coleman[h], P. A. DeYoung[i], A. A. Doetsch[a,c], H. Erington[a,c], T. Gaballah[a,g], N. Gamage[a], E. C. Good[j], B. G. Greaves[h], A. C. Hartley[k], J. Huffman[a,c], C. M. Ireland[a,c], C. Izzo[a], R. Jain[f], J. E. Larsson[l,m,n], R. S. Lubna[a], F. M. Maier[a], M. J. Mogannam[a,b], M. R. Mumpower[o,p], G. Owens-Fryar[a,c], T. H. Ogunbeku[f], D. P. Scriven[a], M. K. Smith[a], C. S. Sumithrarachchi[a], A. Sweet[f], K. Taft[a,c] and M. Wiedeking[q]

[a]*Facility for Rare Isotope Beams, East Lansing, 48823, MI, USA*
[b]*Department of Chemistry, Michigan State University, East Lansing, 48823, MI, USA*
[c]*Department of Physics and Astronomy, Michigan State University, East Lansing, 48823, MI, USA*
[d]*Department of Physics and Astronomy, Ohio University, 45701, Athens, OH, USA*
[e]*Department of Physics and Astrophysics, Central Michigan University, Mt Pleasant, 48859, MI, USA*
[f]*Lawrence Livermore National Laboratory, Livermore, 94550, CA, USA*
[g]*Department of Physics and Astronomy, Mississippi State University, Mississippi State, 39762, MS, USA*
[h]*Department of Physics, University of Guelph, Guelph, N1G 2W1, ON, Canada*
[i]*Department of Physics, Hope College, Holland, 49423, MI, USA*
[j]*Pacific Northwest National Laboratory, Richland, 99354, WA, USA*
[k]*Department of Computer Science, University of Mount Union, Alliance, 44601, OH, USA*
[l]*Institute for Nuclear Physics, Technische Universität Darmstadt, 64289, Darmstadt, Germany*
[m]*GSI Helmholtzzentrum für Schwerionenforschung GmbH, 64291, Darmstadt, Germany*
[n]*Helmholtz Forschungsakademie Hessen für FAIR (HFHF), 64291, Darmstadt, Germany*
[o]*Los Alamos National Laboratory, Los Alamos, 87544, NM, USA*
[p]*Center for Theoretical Astrophysics, Los Alamos, 87544, NM, USA*
[q]*Nuclear Science Division, Lawrence Berkeley National Laboratory, Berkeley, 94720, CA, USA*

ARTICLE INFO

Keywords:
β-decay
NaI(Tl)
$CeBr_3$
Total Absorption Spectroscopy

ABSTRACT

Simulations of astrophysical processes require a plethora of nuclear physics input. In particular, models of neutron-capture nucleosynthesis like the *s*, *i*, and *r* processes require β-decay information and experimentally constrained neutron-capture reaction rates. Past experiments with the 4π Summing NaI(Tl) (SuN) total absorption spectrometer have provided these physics quantities. Here, we outline an upgrade of SuN to SuN++, where 20 new segments (12 NaI(Tl) and 8 $CeBr_3$) have been integrated into the pre-existing SuN total absorption spectrometer to provide increased energy and time resolution in β-decay experiments. The details of the newly upgraded SuN++ total absorption spectrometer are discussed with results from the commissioning experiment at the Facility for Rare Isotope Beams (FRIB) utilizing a ^{70}Cu beam.

1. Introduction

The astrophysical origin of over half of the elements in the universe heavier than iron is largely attributed to neutron-capture nucleosynthesis processes. Nuclear data play a significant role in the calculation of elemental abundances produced by these astrophysical nucleosynthesis processes, and in the absence of experimental measurements, theoretical calculations of nuclear physics quantities are used as model input. Theoretical values often lead to large uncertainties in calculated abundances, notably for the *r* [1] and *i* [2, 3] processes, which occur farther from the valley of stability [4, 5, 6]. Current astrophysical models of *i*-process nucleosynthesis rely heavily on neutron-capture (n,γ)

ORCID(s):

reactions, and the dominating source of uncertainty arising from nuclear physics input in *i*-process nucleosynthesis simulations comes from theoretical predictions of these (n,γ) rates on unstable neutron-rich nuclei [6, 7]. Multiple sensitivity studies have indicated that quantities such as nuclear masses, neutron-capture reaction rates, β-delayed fission, and half-lives all play integral roles in simulations of neutron-capture and β-decay competition in *r*-process nucleosynthesis pathways [4, 5, 8]. Uncertainties in *r*-process abundance patterns from modern simulations persist even when all trajectories for a simulation are combined, further emphasizing the importance of incorporating nuclear data into these simulations [9].

Simulations of the *r* process can be additionally impacted by experimental measurements of β-decay properties, including β-delayed neutron-emission probabilities, half-lives, and β-feeding values [10, 11, 12, 13, 14, 15]. In the cases where experimental information is unavailable, which is common for the neutron-rich isotopes involved in the *r* process, theoretical calculations are used to predict these β-decay properties [16, 17, 18, 19]. Theoretical calculations of β-decay properties are typically benchmarked against known half-lives and β-delayed neutron emission probabilities, which do not fully reflect the β-decay strength of neutron-rich nuclei. A more-direct approach is to compare experimental β-feeding intensity (I_β) values with theory.

I_β values are typically determined from high-resolution γ-ray measurements with high-purity germanium (HPGe) detectors. Such detectors have a low intrinsic efficiency, resulting in weak branching measurements to high-lying states in the child nucleus, causing inflated β-feeding to lower-lying states. This phenomenon is commonly referred to as the Pandemonium effect [20]. More accurate I_β values can be determined by total absorption spectroscopy (TAS), where a large volume, high efficiency detector is used to measure γ rays following β decays [21, 22].

TAS analysis can be performed using a segmented total absorption spectrometer, such as Summing NaI(Tl) total absorption spectrometer (SuN) [23]. The experimental capabilities of SuN to disentangle β-decay information from neutron-rich nuclei far from stability, like those produced at the Facility for Rare Istope Beams (FRIB), is limited by its current segmentation and resolution. Here, we present the details of an upgrade from SuN to the SuN++ total absorption spectrometer, which aims to address these problems. We present the characterization of the upgraded SuN++ calorimeter and details of the commissioning run at FRIB with a beam of ^{70}Cu.

2. The Upgraded Summing NaI(Tl) Total Absorption Spectrometer (SuN++)

2.1. The SuN Total Absorption Spectrometer

The SuN total absorption spectrometer is a 16 inch by 16 inch cylindrical total absorption spectrometer comprised of eight optically isolated NaI(Tl) segments. SuN was originally developed with the purpose of measuring capture reactions on relevant nuclei in astrophysical reactions. Details of the characterization and commissioning of SuN were reported by Simon *et al.* in Ref. [23].

Since its commissioning, SuN has been used to perform total absorption spectroscopy on multiple *r*-process nuclei [24, 25, 26] and to constrain several *i*- and *r*-process neutron-capture reaction rates with the β-Oslo Method [27, 28, 29, 30, 31, 32]. The resolution of SuN (6.1(2)% at 662 keV) [23] significantly limits the ability to build new level schemes when measuring the β decay of exotic nuclei. The limited number of segments in SuN (eight) can also make it difficult to disentangle high-multiplicity cascades. Furthermore, the NaI(Tl) crystals in SuN are sensitive to electrons from β decay, and thus the β-decay electron-induced background detected in SuN can further complicate studies of neutron-rich β-decaying nuclei. In previous and current studies with SuN and SuN++, β-decay electrons have been included in Geant4 simulations of the detectors, and considered in the analysis process.

2.2. The SuN++ Total Absorption Spectrometer

To resolve the aforementioned problems, 20 additional segments (12 NaI(Tl) segments and 8 $CeBr_3$ segments) were added to the original SuN total absorption spectrometer. The $CeBr_3$ segments are meant to improve the timing and energy resolution of the TAS detector to help build level schemes. With the addition of 12 NaI(Tl) segments, the 20 total new segments provide a higher level of segmentation that can be used to differentiate high-multiplicity cascades. Future plans to add electron detectors to the SuN++ system will allow for the capability to track and reject β-decay electrons in the total absorption spectrometer.

The SuN++ upgrade was manufactured by SCIONIX and was developed at FRIB. The eight $CeBr_3$ segments are 152 mm long by 51 mm wide square prisms, enclosed in stretched polytetrafluoroethylene (PTFE) and covered in a 1 mm thick aluminum casing. At the optical interface, a quartz window is optically coupled to a 51 mm diameter Hamamatsu PMT (Model No. R6231) with a head-on type connection. Two different sizes of NaI(Tl) segments were

also included in SuN++, four "large" NaI(Tl) and eight "small" NaI(Tl) segments. The large NaI(Tl) segments are 178 mm long by 102 mm wide square prisms, while the small NaI(Tl) segments are 178 mm long by 51 mm wide square prisms. Each of these detector crystals is also enclosed in stretched PTFE and covered in 1 mm thick aluminum casing. The quartz window in the "small" NaI(Tl) segments is optically coupled to the Model No. R6231 Hamamatsu PMT. The quartz window in the "large" NaI(Tl) segments is optically coupled to a 90 mm diameter Hamamatsu PMT (Model No. R14689), also with a head-on type connection.

On each side of SuN++ relative to the beam direction, ten new segments are inserted between the existing halves of SuN (two large NaI(Tl), four small NaI(Tl), and four $CeBr_3$ detectors), seen in the schematic of SuN++ in Fig. 1. Two large NaI(Tl) segments are located at both ends of the detector. Two small NaI(Tl) segments are stacked upon each other and are placed on the innermost edge of the two large NaI(Tl) segments, followed by four $CeBr_3$ segments that are positioned at the middle of SuN++. This layout is mirrored on the other half of the detector. The naming-scheme for the SuN++ segments is illustrated in Fig. 2.

A schematic of the SuN++ electronics and data acquisition system is shown in Fig. 3. Each of the segments from the original SuN detector is read by three photomultiplier tubes (PMTs) positioned around the segment, giving a total of 24 optically coupled PMTs. All of the new SuN++ segments have individual PMTs that are optically coupled to the crystals. A WIENER MPOD [33] high voltage power supply is used to provide bias voltage to all 44 PMTs. The 24 PMT signals from SuN are sent to a preamplifier and then into the FRIB Digital Data Acquisition System (DDAS) [34]. The 20 photomultiplier signals from SuN++ are fed directly into DDAS. A coincidence condition is set between the three PMTs that comprise each optically isolated segments of the original SuN detector in the digitizer firmware. The SuN++ segments were all high-voltage gain-matched such that the centroids of the 1460 keV ^{40}K peak (from room background) were at the same channel number.

3. Results

3.1. Summing Efficiency and Source Tests

^{137}Cs and ^{60}Co γ-sources were used to test the resolution of the individual segments and the total detection efficiency of the SuN++ total absorption spectrometer. The ^{137}Cs source emits a γ ray at 662 keV, and ^{60}Co emits two γ rays at 1173 and 1332 keV. For the new individual segments of SuN++, the energy resolution values are reported in Fig. 4. The average resolution for the 1332 keV single-γ line from ^{60}Co is 4.65(8)% for the large NaI(Tl), 4.71(16)% for the small NaI(Tl), and 3.38(4)% for the $CeBr_3$ detectors, compared to 5.8(2)% for SuN [23]. To characterize SuN++ and compare its performance to expectations, the Geant4 simulation toolkit was used [35]. This Geant4 simulation was built upon the SuN simulation for β-decay experiments outlined by Dombos *et al.* [24].

The ^{60}Co source was also used to determine the efficiency of detecting a single γ ray at an energy of 1173 keV at the center of SuN++. The single γ-efficiency was experimentally determined to be 71.2(8)%, which agrees within error with the single γ-efficiency determined from Geant4 (70.2(5)%). A typical ^{60}Co total absorption spectrum, sum of segments spectrum, and multiplicity spectrum are shown in Fig. 5(a), (b), and (c), respectively. The total absorption spectrum is made by summing all energy deposited in SuN++ within an event window; this spectrum is related to the excitation energy populated in the child nucleus. The sum-of-segments spectrum is comprised of the sum of histograms of the SuN++ segments (related to the individual γ-rays that de-excite from the child nucleus) which is made by adding the counts in the spectrum from each individual segment together. The multiplicity spectrum shows the number of SuN++ segments that register a signal for each event, related to the number of γ rays involved in a γ-cascade that de-excites from an excitation energy level in the child nucleus. The spectra registered by a large NaI(Tl), small NaI(Tl), and $CeBr_3$ segment are shown in black in panels (d), (e), and (f) in Fig. 5. In all panels, the experimental spectra are shown in black and the Geant4 simulated spectra are shown in red, where excellent agreement between the the Geant4 simulations and the experimental spectra is observed.

A summing efficiency of 51.1(1)% is obtained for a ^{60}Co source located at the center of SuN++. The variation of summing efficiency as a function of source position is illustrated in Fig. 6. In β-decay experiments with SuN++, the implantation point for the ions is at the center position of the total absorption spectrometer, and as such additional Geant4 simulations were performed near the center of the detector to understand the summing efficiency in this region. The efficiency slowly decreases as the source is moved farther away from the center of the detector on both sides, due to the decrease in solid angle covered by the SuN++.

3.2. In-Beam Commissioning of SuN++

The commissioning of SuN++ was performed using a ^{70}Cu beam produced at FRIB at Michigan State University, behind the Low Energy Beam and Ion Trap (LEBIT). A ^{82}Se primary beam of energy 215 MeV/u was impinged on a 4.88 mm thick ^{12}C target. The ^{70}Cu ions were selected by the Advanced Rare Isotope Separator (ARIS) [37], and then passed through a momentum compression beam line and into the gas stopping cell where they were thermalized [38]. ^{70}Cu ions were selected in a dipole mass separator with resolution $\approx$ 1500 and transmitted to the LEBIT 9.4 T Penning trap mass spectrometer at FRIB [39]. The time-of-flight ion-cyclotron-resonance (ToF-ICR) [36, 40] technique was used to detect and quantify the percentage of ground ($J^{\pi}=6^{-}$) and two isomeric ($J^{\pi}=3^{-},1^{+}$) states in the ^{70}Cu beam, as shown by the ToF-ICR spectrum in Fig. 7.

In order to isolate the β decay from the $J^{\pi}=6^{-}$ ground-state of ^{70}Cu within LEBIT, the ions of the two isomers were selectively driven to large radial amplitudes via targeted dipole excitation and removed [41]. The efficiency of this procedure is greater than 90%, based on offline tests using pure samples of $^{39}K^{+}$. The isolated ground-state ions were transmitted to SuN++, where they were implanted on a double-sided silicon strip detector (DSSD) installed downstream of LEBIT. The DSSD consists of 16 horizontal and 16 vertical strips with a width of 1.2 mm. The DSSD output was fed into high-gain preamplifiers, and the β-decay electrons following ^{70}Cu ion implantation were detected with the DSSD. The detected β-decay electrons in the DSSD within threshold were used as a β-tag to generate γ-ray spectra with SuN++. The isolation of the ground-state of ^{70}Cu was confirmed with the β-delayed γ-rays observed in SuN++. The child nucleus of ^{70}Cu (^{70}Zn) is stable.

The total absorption, sum of segments, and multiplicity spectra of ^{70}Zn populated via the β decay of the ^{70}Cu ground-state are shown in the left, middle, and right panels of Fig. 8, respectively. Known levels in ^{70}Zn previously reported by Van Roosbroeck *et al.* were simulated in Geant4 to account for the detector response of SuN++ [43]. The levels in ^{70}Zn populated via the ground-state β decay of ^{70}Cu are known up to 5.06 MeV with the β-decay Q-value (Q_{β}) being 6.584(3) MeV. To account for the apparent feeding shown in Fig. 8 above the last known level in ^{70}Zn, pseudo-levels were created using RAINIER [44]. RAINIER relies on select models for the nuclear level density, γ-ray strength function, and spin distribution, as well as known level schemes at low energies. RAINER is used to simulate decays from a given excitation energy level in the nucleus of interest. The levels simulated with RAINIER are pseudo-levels, which are representative of an energy band that corresponds to the resolution of SuN++. Pseudo-levels in RAINIER were simulated from the highest-known level to the Q_{β} and then fed through the SuN++ Geant4 simulations to account for detector response. A χ^2 minimization procedure was used to simultaneously fit simulated data to all three experimental spectra, and is shown by the red line in Fig. 8; this procedure is similar to those outlined by Dombos *et al.* and Lyons *et al.* [24, 25]. Fig. 8 shows good agreement between the fits and the experimental data.

From the best fits of χ^2-minimization, the I_{β} distribution was extracted. The cumulative I_{β} (%) as a function of excitation energy is shown in Fig. 9. The I_{β} values were compared to the I_{β} obtained from the β-decay of the ground state of ^{70}Cu with SuN [42]. The measurement by Ronning *et al.* [42] (orange error band) agrees with the current measurement (pink error band) within error. Although the cumulative I_{β} values extracted with each detector agree within error, the shape of the β-feeding curves varies slightly between SuN and SuN++. This is likely the result of the improved resolution of SuN++, allowing for better distinction between peaks in the total absorption spectrum and more distributed β-feeding to each excitation energy.

Understanding the multiplicity response of SuN++ is important, as both the original SuN segments and the new SuN++ segments cover restricted azimuthal angles. The multiplicity response of the SuN++ detector to multiplicity (M) = 1, 2, and 3 events is shown in Fig. 10 a. The experimental multiplicities are shown by the colored solid lines, with the Geant4 multiplicity shown by the dashed lines. The M=1 response (magenta) comes from the ^{137}Cs γ-source, the M=2 response (orange) comes from the ^{60}Co γ-source and the M=3 response (blue) comes from the ^{70}Cu β-decay data. The state in ^{70}Zn with the highest I_{β} feeding percentage from ^{70}Cu is at 3038.30(16) keV, which decays by emitting three γ-rays: 1251.7, 901.7, and 884.88 keV. Thus, the peak in the total absorption spectrum at 3038.30(16) keV corresponds to M=3 events. The experimental M=3 spectrum was produced by gating on this TAS peak to produce a multiplicity spectrum, and compared to Geant4 simulations of this level. The Geant4 simulations are in excellent agreement with experimental data.

Fig. 10 b shows the multiplicity response of SuN (purple line) and SuN++ (orange line) to a ^{60}Co source simulated in Geant4. The highest multiplicity that can be registered in SuN is M=8 and the highest multiplicity that can be registered in SuN++ is M=28. We can see in Fig. 10 b that although the multiplicity responses of the two total

absorption spectrometers are not identical, they are very similar, despite the large variation in azimuthal angles of the SuN++ detectors.

4. Conclusions

In this paper, we present the details of the upgrade of SuN to the SuN++ total absorption spectrometer. The summing efficiency of the SuN++ detector was tested using ^{60}Co and ^{137}Cs sources and was found to be 51.1(1)% at 2.5 MeV at the center of SuN++, compared to 65(2)% from SuN [23]. The results obtained from measurements for all detector types were found to be in excellent agreement with GEANT4 simulations. SuN++ was commissioned at FRIB behind LEBIT which delivered isomer-separated beams of ^{70}Cu. The experimentally obtained total absorption, sum-of-segments, and multiplicity spectra were also in good agreement with the simulation for β decay of ^{70}Cu to ^{70}Zn, and with previous results by Ronning *et al.* [42]. SuN++ now allows for better energy resolution and identification of populated states through β decay using the newly added $CeBr_3$ segments, which have an average resolution at 1.332 MeV of 3.38(4)%, compared to 5.8(2)% from the SuN segments. The additional 20 segments in the SuN++ total absorption spectrometer allow for the detection of higher-multiplicity cascades, confirmed by the multiplicity response illustrated in Fig. 10. These upgrades, along with the planned addition of electron detectors to SuN++, are ideal for the investigation of indirect measurements of (n,γ) reactions relevant to *s*-, *i*- and *r*-process nucleosynthesis.

5. Acknowledgments

This material is based upon work supported by the U.S. Department of Energy, Office of Science, Office of Nuclear Physics under Contract No. DE-SC0023633 (MSU) and the National Nuclear Security Administration under Award No. DE-NA0003180 and the Stewardship Science Academic Alliances program under DOE Award No. DOE-DE-NA003906. This work was supported by the National Science Foundation under Grant PHY-209429. This material is based on work supported by NSF Contract No. PHY-2111185. B.P.C acknowledges support from NSF Contract No. PHY-1848177 (CAREER). This work was supported by the Office of Defense Nuclear Nonproliferation Research and Development within the U.S. Department of Energy's National Nuclear Security Administration and performed under the auspices the U.S. Department of Energy by Lawrence Livermore National Laboratory under Contract DE-AC52-07NA27344. This material is based upon work supported by the U.S. Department of Energy, Office of Science, Office of Nuclear Physics under Contract No. DE-AC02-05CH11231 (LBNL). E.C.G. was supported by the Laboratory Directed Research and Development Program at Pacific Northwest National Laboratory operated by Battelle for the U.S. Department of Energy. S.E.C. acknowledges support from the DOE NNSA SSGF under DE-NA0003960. P.A.D acknowledges support from NSF Grant No. PHY-2209138. B.G.G and R.J.C were supported by the Natural Sciences and Engineering Research Council of Canada and the Canadian Foundation for Innovation.

References

[1] F. Käppeler, R. Gallino, S. Bisterzo, W. Aoki, The s process: Nuclear physics, stellar models, and observations, Reviews of Modern Physics 83 (2011) 157.

[2] J. J. Cowan, W. K. Rose, Production of 14C and neutrons in red giants., ApJ 212 (1977) 149–158.

[3] I. U. Roederer, A. I. Karakas, M. Pignatari, F. Herwig, The diverse origins of neutron-capture elements in the metal-poor star HD 94028: Possible detection of products of i-process nucleosynthesis, The Astrophysical Journal 821 (2016) 37.

[4] M. Mumpower, R. Surman, G. McLaughlin, A. Aprahamian, The impact of individual nuclear properties on r-process nucleosynthesis, Progress in Particle and Nuclear Physics 86 (2016) 86–126.

[5] R. Surman, M. Mumpower, R. Sinclair, K. L. Jones, W. R. Hix, G. C. McLaughlin, Sensitivity studies for the weak r process: neutron capture rates, AIP Advances 4 (2014) 041008.

[6] P. Denissenkov, G. Perdikakis, F. Herwig, H. Schatz, C. Ritter, M. Pignatari, S. Jones, S. Nikas, A. Spyrou, The impact of (n,γ) reaction rate uncertainties of unstable isotopes near N=50 on the i-process nucleosynthesis in He-shell flash white dwarfs, Journal of Physics G: Nuclear and Particle Physics 45 (2018) 055203.

[7] S. Martinet, A. Choplin, S. Goriely, L. Seiss, The intermediate neutron capture process - IV. impact of nuclear model and parameter uncertainties, A&A 684 (2024).

[8] D. Martin, A. Arcones, W. Nazarewicz, E. Olsen, Impact of nuclear mass uncertainties on the *r* process, Phys. Rev. Lett. 116 (2016) 121101.

[9] M. R. Mumpower, T. M. Sprouse, J. M. Miller, K. A. Lund, J. C. Garcia, N. Vassh, G. C. McLaughlin, R. Surman, Nuclear uncertainties associated with the nucleosynthesis in ejecta of a black hole accretion disk, The Astrophysical Journal 970 (2024) 173.

[10] P. Hosmer, H. Schatz, A. Aprahamian, O. Arndt, R. R. C. Clement, A. Estrade, K. Farouqi, K.-L. Kratz, S. N. Liddick, A. F. Lisetskiy, P. F. Mantica, P. Möller, W. F. Mueller, F. Montes, A. C. Morton, M. Ouellette, E. Pellegrini, J. Pereira, B. Pfeiffer, P. Reeder, P. Santi, M. Steiner,

A. Stolz, B. E. Tomlin, W. B. Walters, A. Wöhr, Half-lives and branchings for β-delayed neutron emission for neutron-rich Co–Cu isotopes in the r-process, Phys. Rev. C 82 (2010) 025806.

[11] T. Kajino, W. Aoki, A. Balantekin, R. Diehl, M. Famiano, G. Mathews, Current status of r-process nucleosynthesis, Progress in Particle and Nuclear Physics 107 (2019) 109–166.

[12] P. Sarriguren, J. Pereira, β-decay properties of neutron-rich Zr and Mo isotopes, Phys. Rev. C 81 (2010) 064314.

[13] P. Sarriguren, A. Algora, J. Pereira, Gamow-teller response in deformed even and odd neutron-rich Zr and Mo isotopes, Phys. Rev. C 89 (2014) 034311.

[14] K. A. Lund, J. Engel, G. C. McLaughlin, M. R. Mumpower, E. M. Ney, R. Surman, The influence of β-decay rates on r-process observables, The Astrophysical Journal 944 (2023) 144.

[15] J. Chen, J. Y. Fang, Y. W. Hao, Z. M. Niu, Y. F. Niu, Impact of nuclear β-decay half-life uncertainties on the r-process simulations, The Astrophysical Journal 943 (2023) 102.

[16] P. Möller, J. R. Nix, W. D. Meyers, W. J. Swiatecki, Atomic Dat. and Nucl. Dat. Tables 59 (1995) 185–381.

[17] P. Möller, J. Nix, K.-L. Kratz, Nuclear properties for astrophysical and radioactive-ion-beam applications, Atomic Data and Nuclear Data Tables 66 (1997) 131–343.

[18] M. T. Mustonen, J. Engel, Global description of β^- decay in even-even nuclei with the axially-deformed Skyrme finite-amplitude method, Phys. Rev. C 93 (2016) 014304.

[19] T. Marketin, L. Huther, G. Martínez-Pinedo, Large-scale evaluation of β-decay rates of r-process nuclei with the inclusion of first-forbidden transitions, Phys. Rev. C 93 (2016) 025805.

[20] J. Hardy, L. Carraz, B. Jonson, P. Hansen, The essential decay of pandemonium: A demonstration of errors in complex beta-decay schemes, Physics Letters B 71 (1977) 307–310.

[21] J. Tain, D. Cano-Ott, The influence of the unknown de-excitation pattern in the analysis of β-decay total absorption spectra, Nuclear Instruments and Methods in Physics Research Section A: Accelerators, Spectrometers, Detectors and Associated Equipment 571 (2007) 719–727.

[22] A.-A. Zakari-Issoufou, M. Fallot, A. Porta, A. Algora, J. L. Tain, E. Valencia, S. Rice, V. M. Bui, S. Cormon, M. Estienne, J. Agramunt, J. Äystö, M. Bowry, J. A. Briz, R. Caballero-Folch, D. Cano-Ott, A. Cucoanes, V.-V. Elomaa, T. Eronen, E. Estévez, G. F. Farrelly, A. R. Garcia, W. Gelletly, M. B. Gomez-Hornillos, V. Gorlychev, J. Hakala, A. Jokinen, M. D. Jordan, A. Kankainen, P. Karvonen, V. S. Kolhinen, F. G. Kondev, T. Martinez, E. Mendoza, F. Molina, I. Moore, A. B. Perez-Cerdán, Z. Podolyák, H. Penttilä, P. H. Regan, M. Reponen, J. Rissanen, B. Rubio, T. Shiba, A. A. Sonzogni, C. Weber, Total absorption spectroscopy study of ^{92}Rb decay: A major contributor to reactor antineutrino spectrum shape, Phys. Rev. Lett. 115 (2015) 102503.

[23] A. Simon, S. Quinn, A. Spyrou, A. Battaglia, I. Beskin, A. Best, B. Bucher, M. Couder, P. DeYoung, X. Fang, J. Görres, A. Kontos, Q. Li, S. Liddick, A. Long, S. Lyons, K. Padmanabhan, J. Peace, A. Roberts, D. Robertson, K. Smith, M. Smith, E. Stech, B. Stefanek, W. Tan, X. Tang, M. Wiescher, Sun: Summing Nai(Tl) gamma-ray detector for capture reaction measurements, Nuclear Instruments and Methods in Physics Research Section A: Accelerators, Spectrometers, Detectors and Associated Equipment 703 (2013) 16–21.

[24] A. C. Dombos, D.-L. Fang, A. Spyrou, S. J. Quinn, A. Simon, B. A. Brown, K. Cooper, A. E. Gehring, S. N. Liddick, D. J. Morrissey, F. Naqvi, C. S. Sumithrarachchi, R. G. T. Zegers, Total absorption spectroscopy of the β decay of ^{76}Ga, Phys. Rev. C 93 (2016) 064317.

[25] S. Lyons, A. Spyrou, S. N. Liddick, F. Naqvi, B. P. Crider, A. C. Dombos, D. L. Bleuel, B. A. Brown, A. Couture, L. C. Campo, J. Engel, M. Guttormsen, A. C. Larsen, R. Lewis, P. Möller, S. Mosby, M. R. Mumpower, E. M. Ney, A. Palmisano, G. Perdikakis, C. J. Prokop, T. Renstrøm, S. Siem, M. K. Smith, S. J. Quinn, ^{69,71}Co β-decay strength distributions from total absorption spectroscopy, Phys. Rev. C 100 (2019) 025806.

[26] F. Naqvi, S. Karampagia, A. Spyrou, S. Liddick, A. Dombos, D. Bleuel, B. Brown, L. Crespo Campo, A. Couture, B. Crider, T. Ginter, M. Guttormsen, A. Larsen, R. Lewis, P. Möller, S. Mosby, G. Perdikakis, C. Prokop, T. Renstrøm, S. Siem, Total absorption spectroscopy measurement on neutron-rich 74,75Cu isotopes, Nuclear Physics A 1018 (2022) 122359.

[27] A. Spyrou, S. N. Liddick, A. C. Larsen, M. Guttormsen, K. Cooper, A. C. Dombos, D. J. Morrissey, F. Naqvi, G. Perdikakis, S. J. Quinn, T. Renstrøm, J. A. Rodriguez, A. Simon, C. S. Sumithrarachchi, R. G. T. Zegers, Novel technique for constraining r-process (n, γ) reaction rates, Phys. Rev. Lett. 113 (2014) 232502.

[28] S. N. Liddick, A. Spyrou, B. P. Crider, F. Naqvi, A. C. Larsen, M. Guttormsen, M. Mumpower, R. Surman, G. Perdikakis, D. L. Bleuel, A. Couture, L. Crespo Campo, A. C. Dombos, R. Lewis, S. Mosby, S. Nikas, C. J. Prokop, T. Renstrøm, B. Rubio, S. Siem, S. J. Quinn, xperimental neutron capture rate constraint far from stability, Phys. Rev. Lett 116 (2016) 242502.

[29] A. Spyrou, A. C. Larsen, S. N. Liddick, F. Naqvi, B. P. Crider, A. C. Dombos, M. Guttormsen, D. L. Bleuel, A. Couture, L. C. Campo, R. Lewis, S. Mosby, M. R. Mumpower, G. Perdikakis, C. J. Prokop, S. J. Quinn, T. Renstrøm, S. Siem, R. Surman, Neutron-capture rates for explosive nucleosynthesis: the case of 68Ni(n,γ)69Ni, Journal of Physics G: Nuclear and Particle Physics 44 (2017) 044002.

[30] R. Lewis, S. N. Liddick, A. C. Larsen, A. Spyrou, D. L. Bleuel, A. Couture, L. Crespo Campo, B. P. Crider, A. C. Dombos, M. Guttormsen, S. Mosby, F. Naqvi, G. Perdikakis, C. J. Prokop, S. J. Quinn, T. Renstrøm, S. Siem, Experimental constraints on the ^{73}Zn (n,γ)^{74}Zn reaction rate, Phys. Rev. C 99 (2019) 034601.

[31] D. Mücher, A. Spyrou, M. Wiedeking, M. Guttormsen, A. C. Larsen, F. Zeiser, C. Harris, A. L. Richard, M. K. Smith, A. Görgen, S. N. Liddick, S. Siem, H. C. Berg, J. A. Clark, P. A. DeYoung, A. C. Dombos, B. Greaves, L. Hicks, R. Kelmar, S. Lyons, J. Owens-Fryar, A. Palmisano, D. Santiago-Gonzalez, G. Savard, W. W. von Seeger, Extracting model-independent nuclear level densities away from stability, Phys. Rev. C. 107 (2023) L011602.

[32] A. Spyrou, D. Mücher, P. A. Denissenkov, F. Herwig, E. C. Good, G. Balk, H. C. Berg, D. L. Bleuel, J. A. Clark, C. Dembski, P. A. DeYoung, B. Greaves, M. Guttormsen, C. Harris, A. C. Larsen, S. N. Liddick, S. Lyons, M. Markova, M. J. Mogannam, S. Nikas, J. Owens-Fryar, A. Palmisano-Kyle, G. Perdikakis, F. Pogliano, M. Quintieri, A. L. Richard, D. Santiago-Gonzalez, G. Savard, M. K. Smith, A. Sweet, A. Tsantiri, M. Wiedeking, First study of the 139Ba(n,γ)140Ba reaction to constrain the conditions for the astrophysical i process, Phys. Rev. Lett. 132 (2024) 202701.

[33] I. Kontron America, https://www.wiener-d.com/product/mpod-hv-module/, 2025.

[34] C. Prokop, S. Liddick, B. Abromeit, A. Chemey, N. Larson, S. Suchyta, J. Tompkins, Digital data acquisition system implementation at the national superconducting cyclotron laboratory, Nuclear Instruments and Methods in Physics Research Section A: Accelerators, Spectrometers, Detectors and Associated Equipment 741 (2014) 163–168.

[35] S. Agostinelli, J. Allison, K. Amako, J. Apostolakis, H. Araujo, P. Arce, M. Asai, D. Axen, S. Banerjee, G. Barrand, F. Behner, L. Bellagamba, J. Boudreau, L. Broglia, A. Brunengo, H. Burkhardt, S. Chauvie, J. Chuma, R. Chytracek, G. Cooperman, G. Cosmo, P. Degtyarenko, A. Dell'Acqua, G. Depaola, D. Dietrich, R. Enami, A. Feliciello, C. Ferguson, H. Fesefeldt, G. Folger, F. Foppiano, A. Forti, S. Garelli, S. Giani, R. Giannitrapani, D. Gibin, J. Gómez Cadenas, I. González, G. Gracia Abril, G. Greeniaus, W. Greiner, V. Grichine, A. Grossheim, S. Guatelli, P. Gumplinger, R. Hamatsu, K. Hashimoto, H. Hasui, A. Heikkinen, A. Howard, V. Ivanchenko, A. Johnson, F. Jones, J. Kallenbach, N. Kanaya, M. Kawabata, Y. Kawabata, M. Kawaguti, S. Kelner, P. Kent, A. Kimura, T. Kodama, R. Kokoulin, M. Kossov, H. Kurashige, E. Lamanna, T. Lampén, V. Lara, V. Lefebure, F. Lei, M. Liendl, W. Lockman, F. Longo, S. Magni, M. Maire, E. Medernach, K. Minamimoto, P. Mora de Freitas, Y. Morita, K. Murakami, M. Nagamatu, R. Nartallo, P. Nieminen, T. Nishimura, K. Ohtsubo, M. Okamura, S. O'Neale, Y. Oohata, K. Paech, J. Perl, A. Pfeiffer, M. Pia, F. Ranjard, A. Rybin, S. Sadilov, E. Di Salvo, G. Santin, T. Sasaki, N. Savvas, Y. Sawada, S. Scherer, S. Sei, V. Sirotenko, D. Smith, N. Starkov, H. Stoecker, J. Sulkimo, M. Takahata, S. Tanaka, E. Tcherniaev, E. Safai Tehrani, M. Tropeano, P. Truscott, H. Uno, L. Urban, P. Urban, M. Verderi, A. Walkden, W. Wander, H. Weber, J. Wellisch, T. Wenaus, D. Williams, D. Wright, T. Yamada, H. Yoshida, D. Zschiesche, Geant4—a simulation toolkit, Nucl. Instr, and Meth. in Phys. Res. Sec. A 506 (2003) 250–303.

[36] M. König, G. Bollen, H.-J. Kluge, T. Otto, J. Szerypo, Quadrupole excitation of stored ion motion at the true cyclotron frequency, International Journal of Mass Spectrometry and Ion Processes 142 (1995) 95–116.

[37] M. Hausmann, A. Aaron, A. Amthor, M. Avilov, L. Bandura, R. Bennett, G. Bollen, T. Borden, T. Burgess, S. Chouhan, V. Graves, W. Mittig, D. Morrissey, F. Pellemoine, M. Portillo, R. Ronningen, M. Schein, B. Sherrill, A. Zeller, Design of the advanced rare isotope separator aris at frib, Nuclear Instruments and Methods in Physics Research Section B: Beam Interactions with Materials and Atoms 317 (2013) 349–353. XVIth International Conference on ElectroMagnetic Isotope Separators and Techniques Related to their Applications, December 2–7, 2012 at Matsue, Japan.

[38] C. Sumithrarachchi, D. Morrissey, S. Schwarz, K. Lund, G. Bollen, R. Ringle, G. Savard, A. Villari, Beam thermalization in a large gas catcher, Nuclear Instruments and Methods in Physics Research Section B: Beam Interactions with Materials and Atoms 463 (2020) 305–309.

[39] R. Ringle, S. Schwarz, G. Bollen, Penning trap mass spectrometry of rare isotopes produced via projectile fragmentation at the lebit facility, International Journal of Mass Spectrometry 349-350 (2013) 87–93. 100 years of Mass Spectrometry.

[40] G. Bollen, R. B. Moore, G. Savard, H. Stolzenberg, The accuracy of heavy-ion mass measurements using time of flight-ion cyclotron resonance in a Penning trap, Journal of Applied Physics 68 (1990) 4355–4374.

[41] K. Blaum, D. Beck, G. Bollen, P. Delahaye, C. Guénaut, F. Herfurth, A. Kellerbauer, H.-J. Kluge, D. Lunney, S. Schwarz, L. Schweikhard, C. Yazidjian, Population inversion of nuclear states by a Penning trap mass spectrometer, Europhysics Letters 67 (2004) 586.

[42] E. K. Ronning, A. L. Richard, S. N. Liddick, A. Spyrou, I. Yandow, R. Ringle, G. W. Misch, M. R. Mumpower, B. A. Brown, A. Chester, K. Childres, P. DeYoung, J. Owens-Fryar, A. Hamaker, C. Harris, R. Lewis, R. S. Lubna, S. Lyons, M. J. Mogannam, A. Palmisano-Kyle, D. Puentes, T. M. Sprouse, C. S. Sumithrarachchi, M. Wiedeking, Y. Xiao, Total absorption spectroscopy of two isomers in 70Cu influencing nucleosynthesis signatures (2024) Submitted.

[43] J. Van Roosbroeck, H. De Witte, M. Gorska, M. Huyse, K. Kruglov, K. Van de Vel, P. Van Duppen, S. Franchoo, J. Cederkall, V. N. Fedoseyev, H. Fynbo, U. Georg, O. Jonsson, U. Köster, L. Weissman, W. F. Mueller, V. I. Mishin, D. Fedorov, W. B. Walters, N. A. Smirnova, A. Van Dyck, A. De Maesschalck, K. Heyde, Coupling a proton and a neutron to the semidoubly magic nucleus ^{68}Ni: A study of ^{70}Cu via the β decay of ^{70}Ni and ^{70}Cu, Phys. Rev. C 69 (2004) 034313.

[44] L. Kirsch, L. Bernstein, RAINIER: A simulation tool for distributions of excited nuclear states and cascade fluctuations, Nuclear Instruments and Methods in Physics Research Section A: Accelerators, Spectrometers, Detectors and Associated Equipment 892 (2018) 30–40.

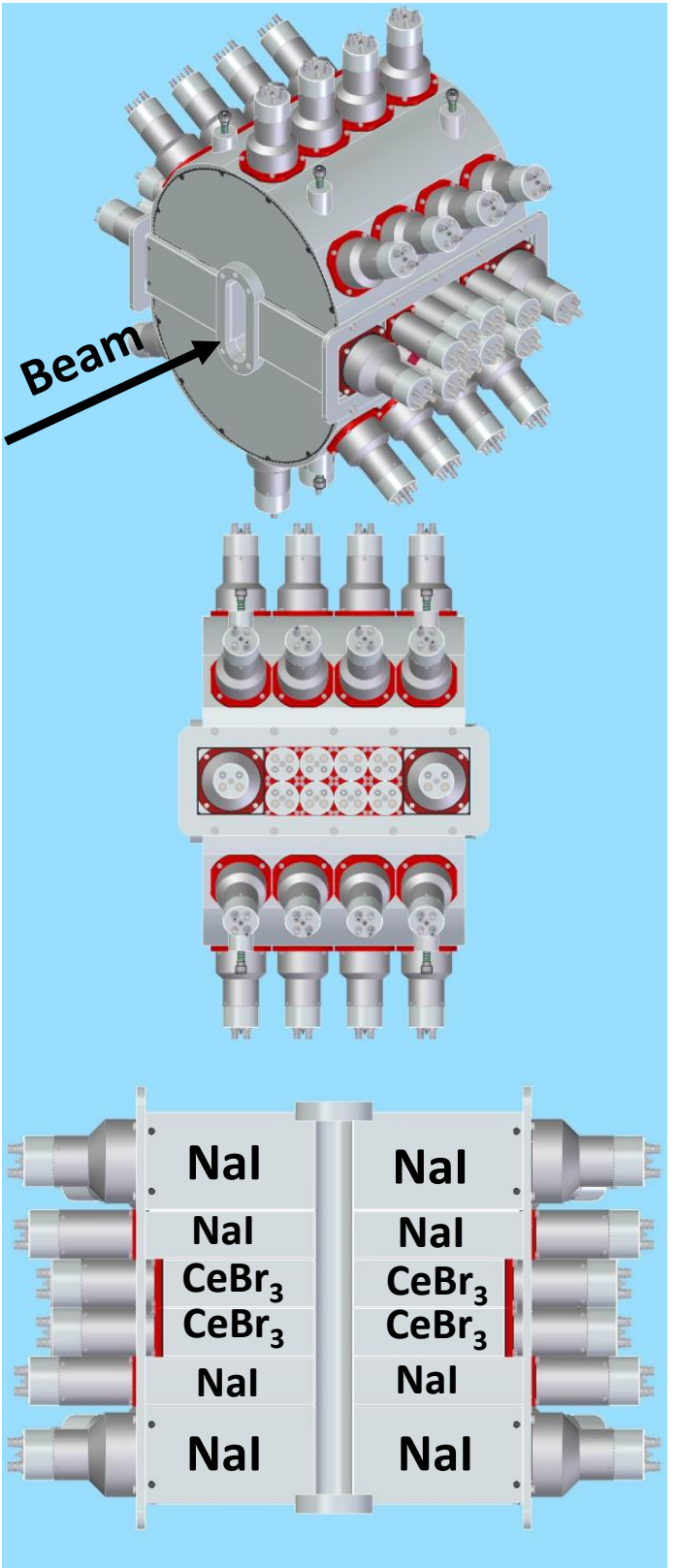

Figure 1: Schematic drawing of the SuN++ detector (a), a side-view (b), and a center-view (c) where the new detector additions can be seen.

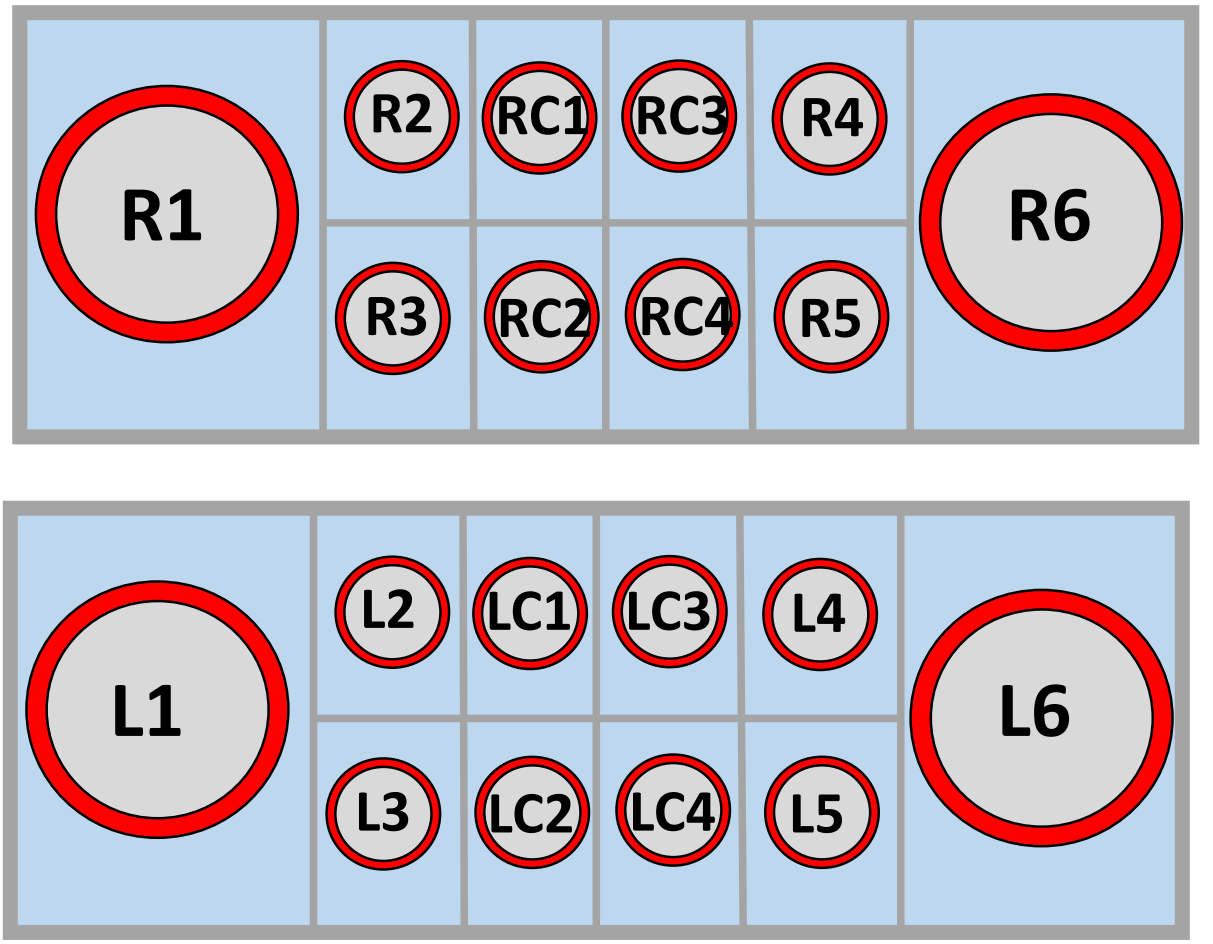

Figure 2: Naming schematic of the SuN++ segments. The detectors on the right side of SuN++ are referred to as "R" detectors and on the left as "L" detectors. A "C" is added before the $CeBr_3$ detector to differentiate them the NaI(Tl) detectors.

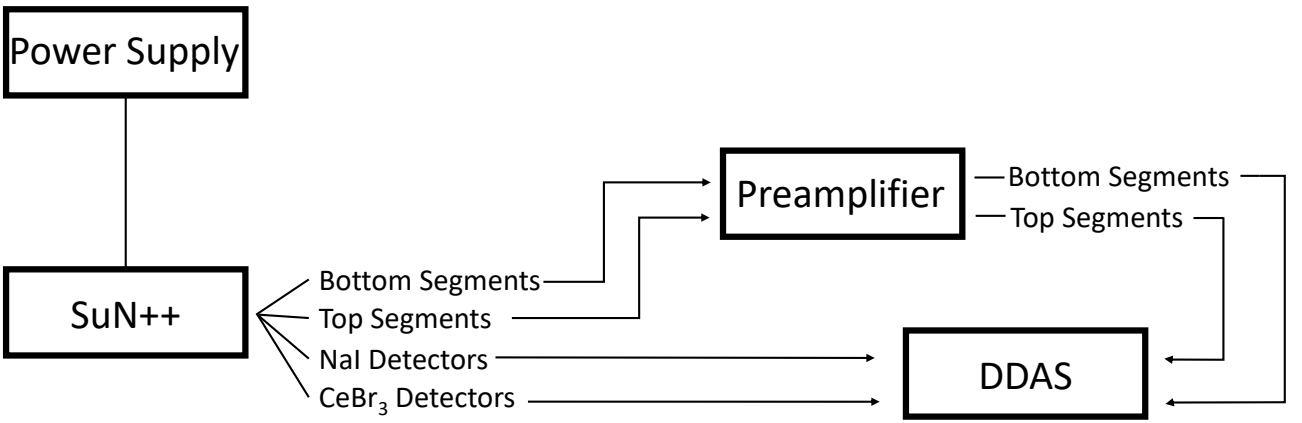

Figure 3: Schematic of the SuN++ electronics. Signals from the original SuN PMTs are sent through a preamplifier before being sent to DDAS. Signals from the new SuN++ detectors are fed directly to DDAS.

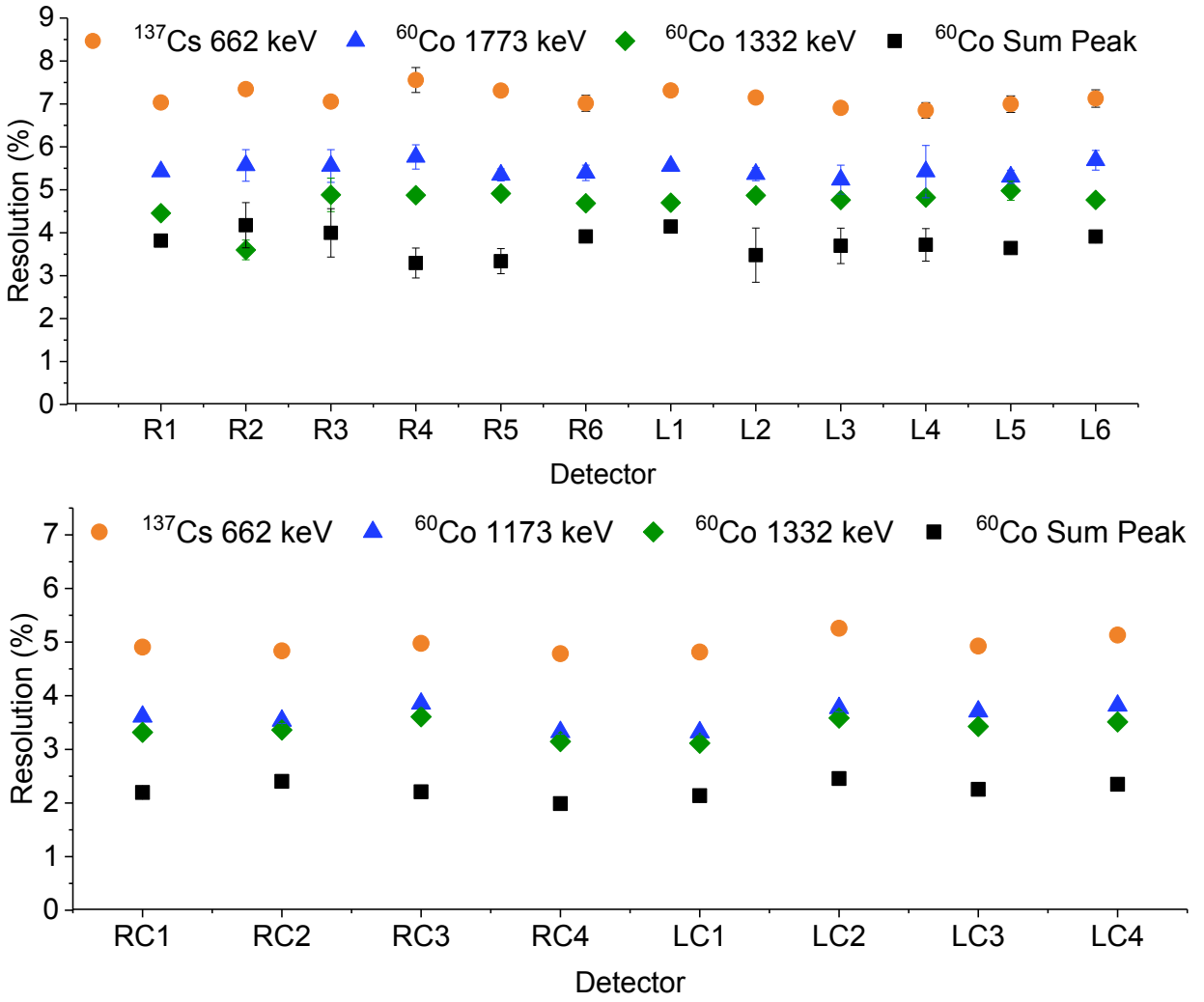

Figure 4: The energy resolution (%) of the new individual SuN++ segments obtained for the ^{60}Co and ^{137}Cs sources. The top panel shows the energy resolution for the NaI(Tl) detectors and the bottom panel shows the energy resolution for the $CeBr_3$ detectors. If error bars are not visible they are within the size of the data points.

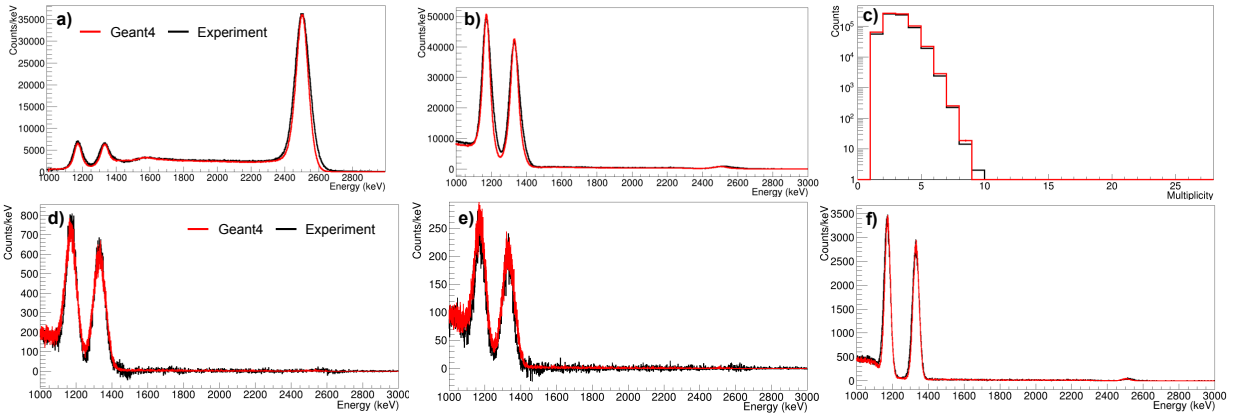

Figure 5: Various spectra from a ^{60}Co γ-source compared to Geant4 simulations of SuN++. Black lines show the experimental data, and Geant4 simulations in red lines. The top panel includes the (a) total absorption, (b) sum of segments, and (c) multiplicity spectra. The bottom panel shows (d) an individual large NaI(Tl) segment, (e) small NaI(Tl) segment, and (f) CeBr3 segment.

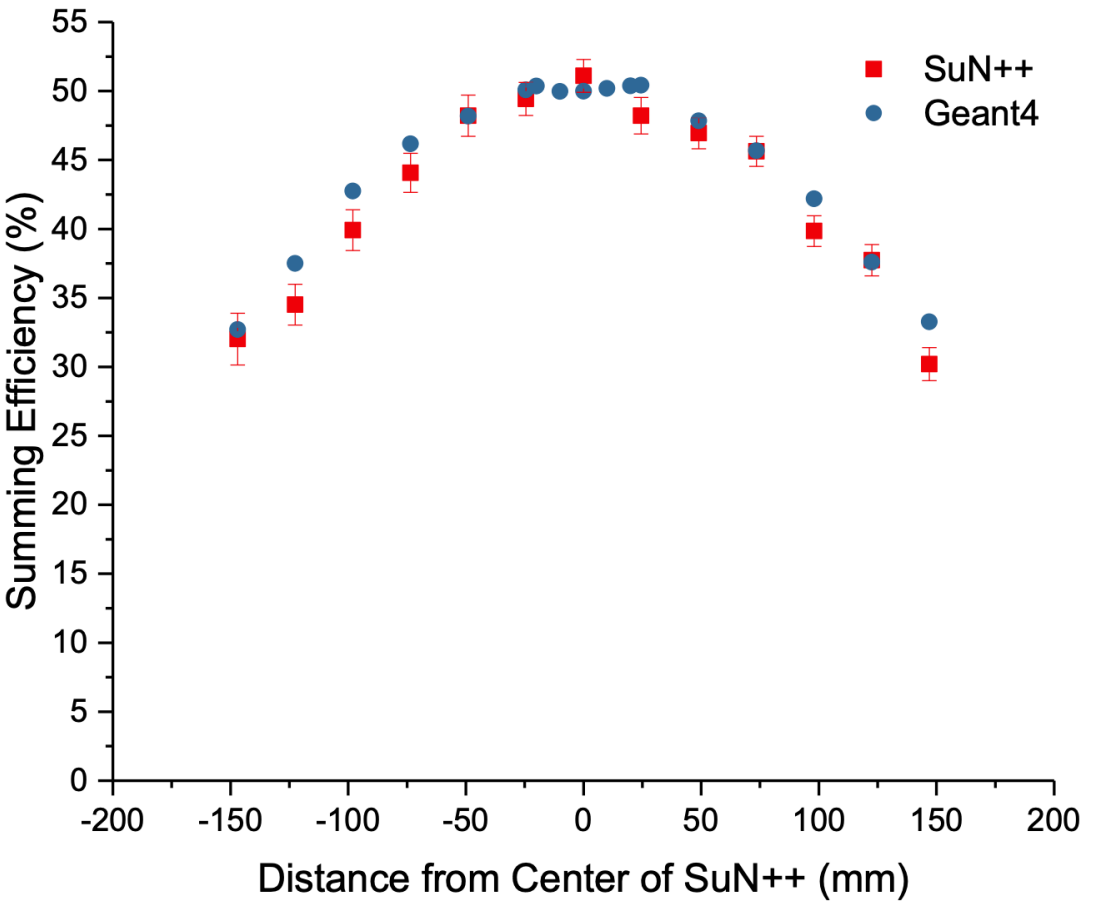

Figure 6: The summing efficiencies (%) calculated from experimental data and Geant4 simulations as a function of position, where the center of SuN++ is at position 0 mm. The experimental data is shown in the red squares and the Geant4 simulations are shown in the blue dots. The error bars associated with the data points are within the size of the data points if they are not visible.

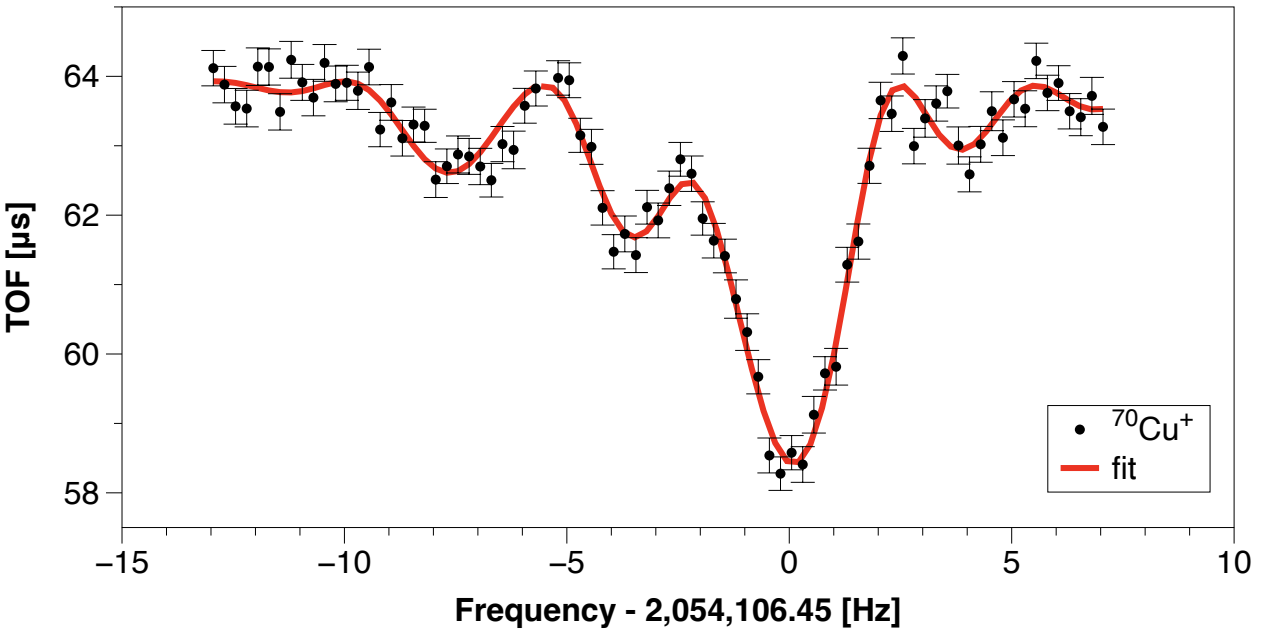

Figure 7: Time-of-Flight Ion Cyclotron Resonance (ToF-ICR) [36] scans from LEBIT when ^{70}Cu was delivered to the Penning trap during the SuN++ commissioning experiment. The figure shows the mix of ground and isomeric states in ^{70}Cu.

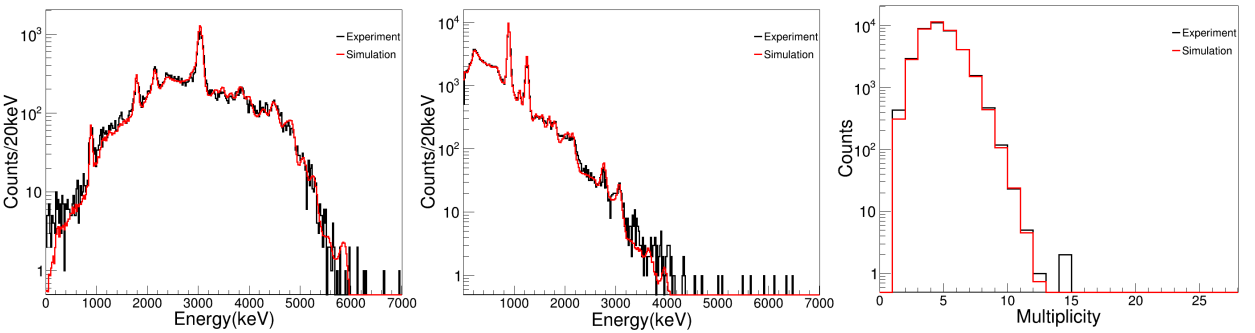

Figure 8: The total absorption spectrum, sum-of-segments, and multiplicity in ^{70}Zn resulting from the ground-state decays of ^{70}Cu.

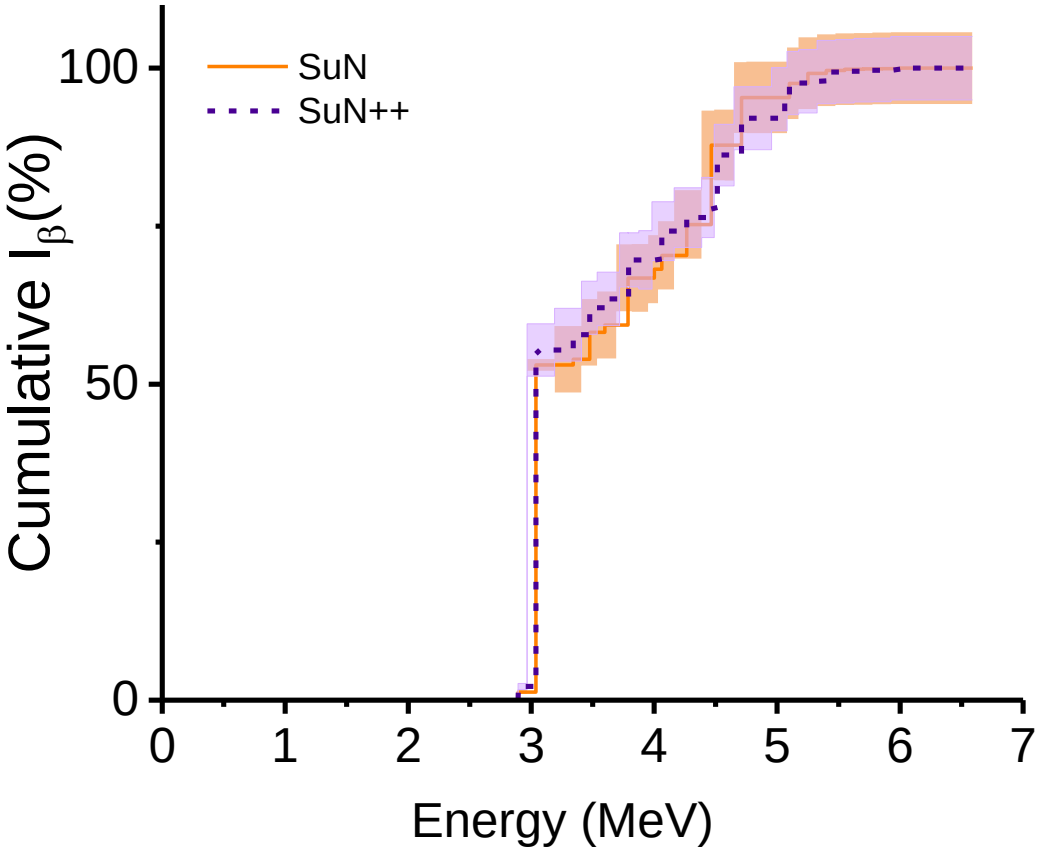

Figure 9: The cumulative β-feeding (I_β) from the β decay of the $J^\pi=6^-$ ground state of ^{70}Cu into ^{70}Zn. The pink band shows the cumulative I_β from SuN++, compared with the cumulative I_β from SuN in orange [42].

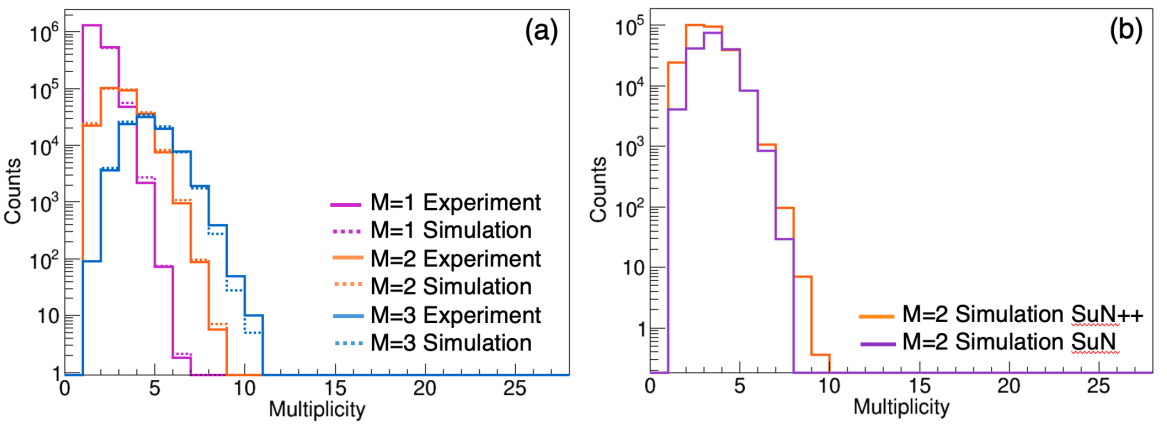

Figure 10: Panel (a) shows the segment multiplicity spectra from SuN++ for γ-ray multiplicity 1 (magenta), 2 (orange), and 3 (blue) events in solid lines compared to Geant4 simulations (dashed lines). Panel (b) shows the segment multiplicity spectra from Geant4 simulations of a ^{60}Co source (M=2) in SuN++ (orange) vs SuN (purple).